Forming Limit Analysis of DP600-800 Steels

M. C. Cardoso, L. P. Moreira

Abstract—In this work, the plastic behaviour of cold-rolled zinc coated dual-phase steel sheets DP600 and DP800 grades is firstly investigated with the help of uniaxial, hydraulic bulge and Forming Limit Curve (FLC) tests. The uniaxial tensile tests were performed in three angular orientations with respect to the rolling direction to evaluate the strain-hardening and plastic anisotropy. True stress-strain curves at large strains were determined from hydraulic bulge testing and fitted to a work-hardening equation. The limit strains are defined at both localized necking and fracture conditions according to Nakajima's hemispherical punch procedure. Also, an elasto-plastic localization model is proposed in order to predict strain and stress based forming limit curves. The investigated dual-phase sheets showed a good formability in the biaxial stretching and drawing FLC regions. For both DP600 and DP800 sheets, the corresponding numerical predictions overestimated and underestimated the experimental limit strains in the biaxial stretching and drawing FLC regions, respectively. This can be attributed to the restricted failure necking condition adopted in the numerical model, which is not suitable to describe the tensile and shear fracture mechanisms in advanced high strength steels under equibiaxial and biaxial stretching conditions.

Keywords—Advanced high strength steels, forming limit curve, numerical modeling, sheet metal forming.

I. INTRODUCTION

THE automotive sector plays an important role in the technological development process of the global economy. As a result, environmental requirements increased mainly with respect to the reduction of vehicle emissions which causes greenhouse effects. A way to meet this requirement is to reduce the fuel consumption by decreasing the mass vehicle. In this context, in order to reduce the mass of the vehicles recently proposed automotive industry solutions have been focused on the use of advanced high strength steels, replacement of some steel parts by aluminium and magnesium alloys, and use of polymers and glass-fiber composites. According to [1] about 70% of an automobile mass is made of steel and, hence, reducing the steel mass will optimize the vehicle mass reduction. To deal with the increasing use of lightweight materials, the steel industry focused on the development of advanced high strength steels (AHSS), which can meet requirements for car safty, namely, front or rear collision and, hence, help to preserve the passenger compartment. Most of the structural automotive components manufactured by sheet metal forming is shaped with the aid of a punch-die tooling to obtain a desired component geometry. Therefore, the formability analysis of

AHSS is essential for the correct use of these new steels grades in stamping processes. Firstly introduced in [2] and extended later in [3], the Forming Limit Diagram (FLD) concept is a very important tool in the design process and try-out steps to obtain a stamped sheet metal part without any failure due to localized necking and tearing. The FLD is defined in the axes of minor (ε_2) and major (ε_1) principal strains measured in the workpiece surface. The curve defined by plotting the corresponding limit strains determined for linear strain-paths is the Forming Limit Curve (FLC). The use of the FLC in the press shop help to define a process safe window which separates safe and necking regions in a stamped part and it is to evaluate the level of deformation that a sheet metal can withstand in a forming process. The prediction of the forming limits set by the occurrence of localized necking in plastically stretched sheets has been the subject of a very large number of theoretical and numerical analyses. Hill [4] proposed an instability criterion to forecast the localized necking in thin metal sheets under plane-stress conditions. Nevertheless, Hill's criterion predicts only localized plastic deformation in the negative minor strain region of the FLC ($\varepsilon_2 < 0$). In order to cover both the drawing ($\varepsilon_1 > 0$ and $\varepsilon_2 < 0$) and biaxial stretching ($\varepsilon_1 > 0$ and $\varepsilon_2 > 0$) FLC regions, [5] proposed a plane-stress model with an initial imperfection zone in the sheet thickness. The original Marciniak and Kuczynski theoretical model, hereafter referred to as M-K model, assumes the imperfection zone in the form of a groove which is perpendicular to the major in-plane principal stress (σ_1, σ_2). Almost all the available phenomenological descriptions of plastic yielding have been implemented in such a simple M-K analysis involving the existence of two individual zones, namely, the homogeneous zone, and the defective, thinner zone. However, most of the available proposed M-K models neglected the elastic strains components assuming rigid-plastic together with nonlinear work-hardening. This work aims to extend the original M-K model to account for the elastic strains in order to forecast the limit strains of two AHHS steels, namely, dual-phase (DP) cold-rolled zinc coated DP600 and DP800 sheets 1.2 mm nominal thickness. The experimental test procedures adopted to evaluate the plastic behaviour and the FLC of both DP600 and DP800 sheets are firstly detailed. Next, the M-K model governing equations are recalled and the limit strains predictions are compared to the experimental FLC. Also, the corresponding Forming Limit Stress Curve (FLSC) are discussed in comparison to the experimental uniaxial ultimate yield strength values of DP600 and DP800 steels.

M. C. Cardoso and L. P. Moreira are with the Universidade Federal Fluminense, Volta Redonda, Rio de Janeiro State, ZIP code 27255-125, Brazil (Phone: +55-24-21-07-3730; Fax:+55-24-21-07-3742 e-mail: marcelocardoso @metal.eeimvr.uff.br, luciano.moreira@metal.eeimvr.uff.br).

World Academy of Science, Engineering and Technology
International Journal of Materials and Metallurgical Engineering
Vol:9, No:9, 2015

II. EXPERIMENTAL PROCEDURE

A. Uniaxial Tensile Test

The uniaxial tensile tests to evaluate the mechanical properties and plastic anisotropy of DP600 and DP800 steels were performed with the INSTRON model 5582 universal machine equipped with a 30 kN load cell and an advanced video extensometer to measure both longitudinal and width strains. The mechanical properties were evaluated from 3 specimens taken at 0º, 45º and 90º orientations with respect to the rolling direction (RD). A cross-head rate equal to 1.8 mm/min was kept up to the yield stress and then increased to 10 mm/min up to specimen failure. The yield stress was defined at 0.2% plastic strain whereas the strain-hardening exponent was obtained from the true-strain range between 0.1 and 0.2. The plastic anisotropy coefficients or the Lankford r-values were determined using an automatic calculation using a least-squares method by fitting the video-recorded specimen width and length strains data between 0.2% and the uniform strain defined at maximum load. The uniaxial tensile specimens were machined by CNC milling according to the geometry and dimensions shown in Fig. 1.
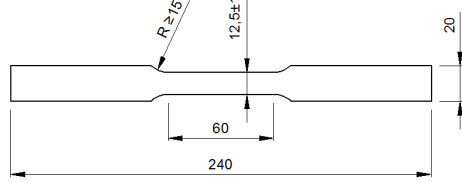

Fig. 1 Uniaxial tensile specimen geometry and dimensions (mm)

B. Hydraulic Bulge Test

Hydraulic bulge tests were performed with the Erichsen model 145-60 universal machine using a constant blank-holder load of 500 kN and a constant forming speed of 60 mm/min. Three blank specimens were machined with 180 mm diameter and tested for each DP steel sheet grade. The specimen strains were obtained from an electrochemically etched 2.5 mm square grid pattern using an automatic digital image correlation (DIC) device system. Bulge curvature was determined from the dome height measurements according to the Hill's analysis [6], [7]. The equibiaxial flow stress was calculated from the membrane theory while the equivalent plastic strain is defined according to the von Mises isotropic yield criterion, wherein the dome apex thickness plastic strain was calculated assuming the plastic incompressibility condition. For the M-K modelling purposes, the flow curves determined from the bulge tests were fitted to Swift work-hardening equation defined as:

$$\sigma = K(\varepsilon_0 + \varepsilon^p)^n \qquad (1)$$

where K is the strength coefficient (MPa), ε_0 is the pre-strain and n is the strain-hardening exponent.

C. Forming Limit Curve (FLC) Test

Nakajima's procedure with 100 mm hemispherical punch diameter was adopted to determine the Forming Limit Curve (FLC) of dual-phase steel grades DP600 and DP800. The FLC tests were performed with the Erichsen model 145-60 universal machine using a constant blank-holder load of 500 kN and a constant forming speed of 60 mm/min. The limit strains at the necking condition were defined as per ISO 12004-2:2008 standard with the help of a DIC system, in which a set of four CCD cameras records in-situ the displacements from a 2.5 mm square grid pattern previously electrochemically etched to the specimen surface. The AutoGrid® in-process DIC system was used to record in-situ the surface strains. Fig. 2 shows the blank geometries and dimensions adopted in order to cover roughly both the drawing ($\varepsilon_1 > 0$ and $\varepsilon_2 < 0$) and biaxial stretching ($\varepsilon_1 > 0$ and $\varepsilon_2 > 0$) FLC regions. The blank diameter which is equal to 220 mm was taken at 90 degrees with respect to the sheet rolling direction. The lubrication between the punch and the blank consisted of a PVC disk with 50 mm diameter and 5 mm thick, two Teflon® layers with 50 mm diameter and 0.05 mm thick and Vaseline. For the each geometry at least three blanks were tested to obtain the complete FLC.
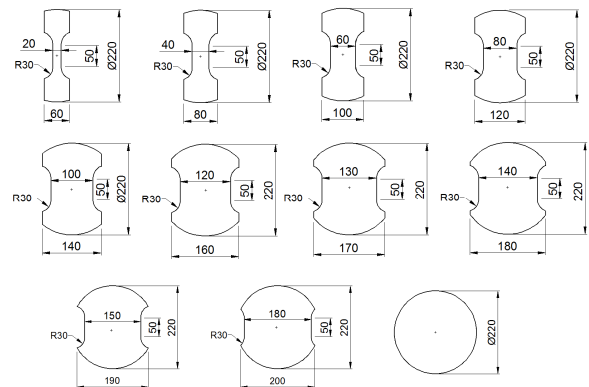

Fig. 2 Forming Limit Curve blank geometries and dimensions (mm)

According to the ISO 12004-2:2008 standard procedure, firstly at least three intersections lines nearly perpendicular to the fracture, as indicated in the contour plot shown in Fig. 3, must be drawn to plot the true major and minor surface principal strains distributions on both sides of the specimen fracture site. For each intersection line, the corresponding true strains are plotted as function of the grid position in order to discard the point nodes which are subjected to the localized necking. Then, a border area is obtained by calculating the local second derivatives from a parabola fitting of each major and minor true strains located at left and right sides of the fracture. Secondly, the remaining nodes, including the ones on either sides of the border necking area, are used to fit a 6th order polynomial. Finally, the peak strain node location is replaced in the fitted 6th order polynomial to define the major and minor limit strains of the corresponding intersection line. This procedure is then repeated for the each blank specimen geometry from which both the major and minor limit strains are defined as the averaged values of the selected sections.

World Academy of Science, Engineering and Technology
International Journal of Materials and Metallurgical Engineering
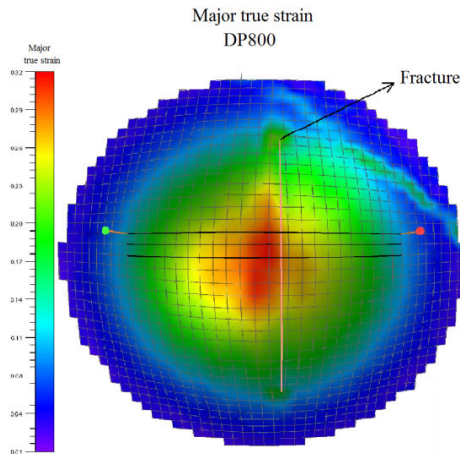Vol:9, No:9, 2015

Fig. 3 Major true strain contour plot of a deformed DP800 specimen: in detail the three selected sections perpendicular to the fracture site

The limit strains at the fracture condition were determined with the help of the ASAME® target model, schematically shown in Fig. 4, according to a similar procedure in which the fracture limit strains are obtained from the image reconstruction of the fractured zone.
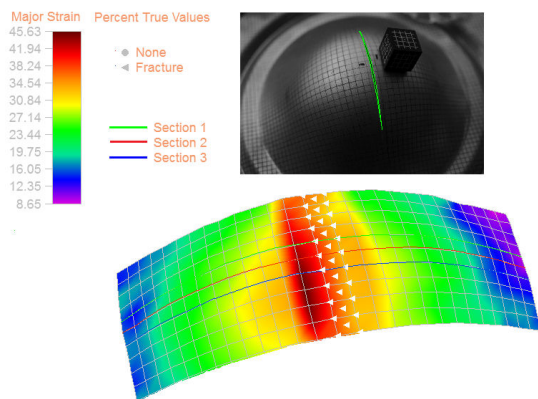

Fig. 4 Fractured DP800 specimen with a target and corresponding major strain contour plot with sections perpendicular to the fracture

III. MARCINIAK-KUCZYNSKI MODEL

The M-K model is based upon the existence of an initial imperfection across the thickness, as depicted in Fig. 5, where the superscripts "a" and "b" denote the homogeneous and the defective zones, respectively. The coordinate system is defined by a common frame $(O, \boldsymbol{n}, \boldsymbol{t}, \boldsymbol{z})$ in which $\boldsymbol{n}$ and $\boldsymbol{t}$ are the normal and tangential directions to the imperfection whereas $\boldsymbol{z}$ is the in-plane normal axis of orthotropy symmetry. The imperfection has an initial angular orientation defined by the angle between the in-plane axes of material orthotropic symmetry $(\boldsymbol{x}^a, \boldsymbol{y}^a)$ and the $(\boldsymbol{n}, \boldsymbol{t})$ directions, to be exact, $\psi = (\boldsymbol{x}^a, \boldsymbol{n}) \equiv (\boldsymbol{y}^a, \boldsymbol{t})$, which rotation as a function of the principal plastic strain increments $(d\varepsilon_1^a, d\varepsilon_2^a)$ in the homogeneous zone is defined as:

$$\mathrm{tg}(\psi + d\psi) = \mathrm{tg}(\psi)[(1 + d\varepsilon_1^a)/(1 + d\varepsilon_2^a)] \qquad (2)$$

The in-plane orthotropy axes are assumed to coincide with the in-plane principal stress directions in the homogeneous zone, i.e., $\boldsymbol{x}^a \equiv \boldsymbol{1}^a$ and $\boldsymbol{y}^a \equiv \boldsymbol{2}^a$. However, the orthotropy symmetry axes do not coincide with the principal stress directions $(\boldsymbol{1}^b, \boldsymbol{2}^b)$ in the imperfection zone "b", that is to say, the angle $\varphi = (\boldsymbol{x}^b, \boldsymbol{1}^a) \equiv (\boldsymbol{y}^b, \boldsymbol{2}^a)$ in Fig. 5 rotates in a corotational frame as detailed in [8].

The initial value of the geometrical imperfection is defined by the ratio between the initial thickness values of the imperfection zone and homogeneous zone, that is, $f_0 = t_0^b / t_0^a$. The current geometrical imperfection is obtained as a function of the total strains across the sheet thickness in both zones "a" and "b":

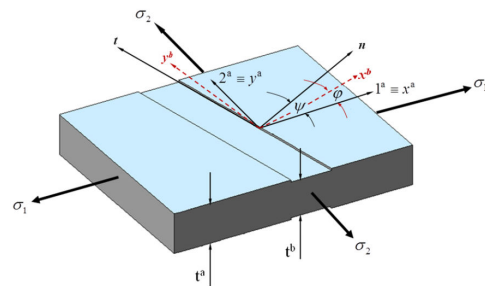$$f = f_0 \exp(\varepsilon_{zz}^b - \varepsilon_{zz}^a) \qquad (3)$$

Fig. 5 Schematic of the M-K model [8]

The M-K governing equations are defined by the force equilibrium between the two model zones along the normal $\boldsymbol{n}$ and tangential $\boldsymbol{t}$ directions with respect to the geometrical imperfection:

$$\begin{aligned} F_{nn}^a &= F_{nn}^b \\ F_{nt}^a &= F_{nt}^b \end{aligned} \qquad (4)$$

together with the compatibility condition which imposes that the strain increments along the tangential direction $\boldsymbol{t}$ must be the same between the zones "a" and "b", namely, $d\varepsilon_{tt}^a = d\varepsilon_{tt}^b$. The solution of the M-K model is firstly obtained imposing an elastic prediction step defined by Hooke's linear isotropic elasticity law assuming a fixed strain-ratio prescribed in the homogeneous zone between the minor and major in-plane principal strain increments, given by $\rho^a = d\varepsilon_2^a / d\varepsilon_1^a$. Secondly, by loading the homogeneous zone with a small value of the major in-plane principal strain increment, usually $d\varepsilon_1^a = 10^{-4}$. This elastic prediction step provides a trial stress state which is obtained from an initial or old stress state as:

$$\sigma_{ij}^{Trial} = \sigma_{ij}^{Old} + C_{ijkl}^e \Delta \varepsilon_{kl} \qquad (5)$$

where C_{ijkl}^e is the 4th order linear isotropic elasticity tensor which can be defined as a function of the Young modulus, E, and the Poisson's coefficient, ν.

Next, the elasto-plastic loading condition must be checked to verify whether the trial stress state defined in (5) satisfies the conditions defined with the yield function:

World Academy of Science, Engineering and Technology
International Journal of Materials and Metallurgical Engineering
Vol:9, No:9, 2015

$$f\left(\sigma_{ij}^{Trial}, \bar{\varepsilon}^{Old}\right) = F\left(\sigma_{ij}^{Trial}\right) - \bar{\sigma}\left(\bar{\varepsilon}^{Old}\right) \geq 0 \qquad (6)$$

in which the isotropic work-hardening assumption is assumed with the associated plastic flow theory and nonlinear strain-hardening defined as a function of the effective plastic strain, $\bar{\sigma} = \bar{\sigma}(\bar{\varepsilon})$, and $F\left(\sigma_{ij}^{Trial}\right)$ is a first order homogeneous stress function. If the conditions in (6) are not verified then the current trial stress state provides an elastic loading or unloading and, thus, all the stress and strain components are defined from the elastic prediction step. Otherwise, a plastic correction step must be performed to calculate the stress components as well as elastic and plastic strain increments in both homogeneous and defective model zones. Owing to the plastic incompressibility condition, verified when most metals do not exhibit any phase changes, the plastic correction is obtained as:

$$\sigma_{ij}^{New} = \sigma_{ij}^{Trial} - 2\mu\Delta\varepsilon_{ij}^{p} \qquad (7)$$

In (7) $\mu = E/2(1 + v)$ is the shear modulus whereas $\Delta\varepsilon_{ij}^{p}$ are the plastic strain increments defined from the associated plastic flow-rule:

$$\Delta\varepsilon_{ij}^{p} = \Delta\bar{\varepsilon}^{p} \frac{\partial F\left(\sigma_{ij}^{Trial}\right)}{\partial\sigma_{ij}^{Trial}} \qquad (8)$$

It is worth to note that the only unknown in (7) is the effective plastic strain increment $\Delta\bar{\varepsilon}^{p}$, since the partial derivatives of the stress function $F(\sigma_{ij})$ are calculated from the trial stress state. An appropriate procedure to define the effective plastic strain increment consists of calculating the increment of the plastic work:

$$\sigma_{ij}^{New}\Delta\varepsilon_{ij}^{p} = \bar{\sigma}^{New}\Delta\bar{\varepsilon}^{p} \qquad (9)$$

with the updated stress components σ_{ij}^{New}, defined in (7), and the associated flow rule in (8), to obtain a nonlinear function of the effective plastic strain increment as:

$$\left(\sigma_{ij}F_{,ij}\right)^{Trial}\left[1 - \frac{2\mu\left(F_{,ij}F_{,ij}\right)^{Trial}}{\left(\sigma_{kl}F_{,kl}\right)^{Trial}}\Delta\bar{\varepsilon}^{p}\right] - \bar{\sigma}^{New} = 0 \qquad (10)$$

in which $\bar{\sigma}^{New}$ is the updated effective stress measure. Besides, it is worth to observe that the root in (10) is bracketed between $\Delta\bar{\varepsilon}^{p} = 0$ and a upper limit value defined as:

$$\Delta\bar{\varepsilon}^{p} = \frac{\left(\sigma_{kl}F_{,kl}\right)^{Trial}}{2\mu\left(F_{,ij}F_{,ij}\right)^{Trial}} \qquad (11)$$

The remaining unknowns in the imperfection M-K model zone "b" $\mathbf{X} = \left[\Delta\varepsilon_{nn}^{b}\ \Delta\varepsilon_{nt}^{b}\right]^{T}$ are then numerically calculated from the stress and strain states in the homogeneous zone "a". The solution is then obtained by rewriting the equilibrium force conditions in (4) as a set of two nonlinear equations:

$$\begin{aligned} F_1 &= f\frac{\sigma_{nn}^{b}}{\sigma_{nn}^{a}} - 1 \\ F_2 &= f\frac{\sigma_{nt}^{b}}{\sigma_{nt}^{a}} - 1 \end{aligned} \qquad (12)$$

which is solved using the Newton's method where the initial guess for the solution vector is set to the values obtained in the homogeneous zone $\mathbf{X_0} = [\Delta\varepsilon_{nn}^{a}\ \Delta\varepsilon_{nt}^{a}]^{T}$.

The localized necking criterion can then be defined when both ratios $\Delta\varepsilon_{nn}^{b}/\Delta\varepsilon_{nn}^{a} \geq 50$ and $\Delta\varepsilon_{nt}^{b}/\Delta\varepsilon_{nt}^{a} \geq 50$ are satisfied. Next, the limit strains are obtained as the corresponding accumulated principal strains in the homogeneous zone "a", namely the data pair($\varepsilon_1^{a,*}, \varepsilon_2^{a,*}$), by the minimum values of the major principal strains obtained as a function of the geometrical imperfection orientation angle ψ, which, in turn, is varied between 0 and 90 degrees. Finally, the complete FLC prediction is obtained by varying the strain-ratio in the homogeneous zone, namely, $\rho^a = \Delta\varepsilon_2^a/\Delta\varepsilon_1^a$, between the FLC drawing region ($\rho^a = -0.5$) and the equibiaxial straining mode ($\rho^a = 1$). Also, the corresponding Forming Limit Stress Curve (FLSC) predictions are obtained from the principal stress values in the homogeneous zone between the uniaxial tensile stress-state ($\sigma_1^a \neq 0, \sigma_2^a = 0$) and the equibiaxial straining mode ($\rho^a = 1$).

The plane-stress orthotropic plasticity criterion proposed by Ferron et al. [9] is adopted to describe the plastic anisotropy behaviour of both dual-phase steels DP600 and DP800 grades. For numerical implementation purposes, Ferron's orthotropic yield function is cast as [10]:

$$f = \Phi(x_1, x_2, \varphi) - \bar{\sigma} \qquad (13)$$

In (13) $x_1 = (\sigma_1 + \sigma_2)/2$ and $x_1 = (\sigma_1 - \sigma_2)/2$ denote the centre and the radius of Mohr's circle, respectively, whereas the angle φ defines the orientation between the in-plane principal stress axes (1,2) and in-plane orthotropy directions (x, y), i.e., $\varphi = (1, x) \equiv (2, y)$. In Ferron's orthotropic plasticity criterion, the effective stress measure $\bar{\sigma}$ is identified as the equibiaxial yield stress($\sigma_1 = \sigma_2 = \sigma_b$). The first order stress function $\Phi(x_1, x_2, \varphi)$ is defined as [10]:

$$\Phi = \left\{ \begin{array}{l} \left[\dfrac{\left(x_1^2 + Ax_2^2\right)^3 - kx_1^2\left(x_1^2 - Bx_2^2\right)^2}{(1-k)}\right]^{m/6} \\[2mm] -\dfrac{2a}{(1-k)^{m/6}}\dfrac{x_2 x_1^{2n-1}}{\left(x_1^2 + x_2^2\right)^{n-m/2}}\cos 2\varphi \\[2mm] +\dfrac{b}{(1-k)^{m/6}}\dfrac{x_2^{2p}}{\left(x_1^2 + x_2^2\right)^{p-m/2}}(\cos 2\varphi)^{2q} \end{array} \right\}^{\frac{1}{m}} \qquad (14)$$

In (14) the exponents m, n, p and q are positive integers whereas A, B, k, a and b are material parameter which can be calculated in two steps. Firstly, assuming $B = 3A$ and imposing a positive k-value, which allows a flattening of the yield surface between the plane-strain tension/compression and pure shear stress states, the parameter A is calculated from the Lankford R-value at 45 degrees with respect to the rolling direction (RD). The recommended values for the exponents in (4) are $m = 2$, $n = 1$ or 2, $p = 1$ or 2 and $q = 1$, as explained

World Academy of Science, Engineering and Technology
International Journal of Materials and Metallurgical Engineering
Vol:9, No:9, 2015

in detail in [9]. Then, the material parameters a and b describing the initial in-plane anisotropy can be determined from the Lankford R-values at 0 and 90 degrees [9]. In this work, the parameter k-values are set equal to 0.2 and 0.3 for the DP600 and DP800 steels, respectively. The exponents in (14) were set defined for both DP600 and DP800 sheets as $m = n = p = 2$ and $q = 1$.

IV. RESULTS AND DISCUSSION

A. Uniaxial Mechanical Properties

The average values of the mechanical properties of steel DP600 sheet are listed in Table I, in which the italic values are the corresponding standard deviations obtained from three tests for each angular orientation with respect to the rolling direction. Both the yield stress (σ_y) and ultimate tensile strength (σ_u) values exhibited the same angular orientation evolution, that is, $\sigma_{90} > \sigma_0 > \sigma_{45}$, which is consistent with the highest plastic anisotropy coefficient at 45 degrees orientation with respect to the rolling direction. The average normal plastic anisotropy is $\bar{R} = (R_0 + 2R_{45} + R_{90})/4 = 0.925$. The uniaxial tensile true stress-strain curves of DP600 are plotted in Fig. 6 where it can be observed that both uniform (ε_u) and total (ε_T) strain values provided the same angular evolution, namely, $\varepsilon_{45} > \varepsilon_0 > \varepsilon_{90}$, which is in agreement with the yield strength behaviour.

TABLE I
UNIAXIAL MECHANICAL PROPERTIES OF DP600 STEEL SHEET

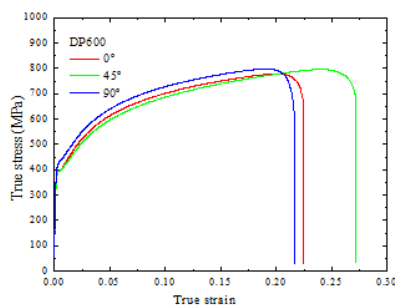| Orientation (degrees)	σ_y (MPa)	σ_u (MPa)	ε_u (%)	ε_T (%)	n	R
0	392.24	748.64	15.2	22.6	0.201	0.516
	4.05	7.28	0.3	0.3	0.002	0.033
45	385.64	750.50	17.4	26.8	0.218	1.237
	2.84	7.49	0.1	1.4	0.008	0.042
90	421.85	774.25	14.9	21.8	0.194	0.711
	4.94	11.13	0.1	0.9	0.002	0.011

Fig. 6 Uniaxial tensile true stress-strain curves of DP600 steel

Table II lists the uniaxial mechanical properties obtained for the DP800 steel, which also exhibits the same yield stress and ultimate yield strength orientation dependence as DP600 grade, $\sigma_{90} > \sigma_0 > \sigma_{45}$, with the ductility behaviour, $\varepsilon_{45} > \varepsilon_0 > \varepsilon_{90}$. The average normal plastic anisotropy obtained for the DP800 steel grade is $\bar{R} = 0.857$. Due to the higher martensite content, DP800 steel sheet exhibits improved ultimate yield strength in detriment to the uniform strain and

strain-hardening exponent values. The corresponding uniaxial tensile true stress-strain curves are shown in Fig. 7 where it is worth to observe a remarkable plastic behaviour difference at 90 degrees angular orientation in comparison with the uniaxial tensile stress-strain curves obtained at 0 and 45 degrees.

TABLE II
UNIAXIAL MECHANICAL PROPERTIES OF DP800 STEEL SHEET

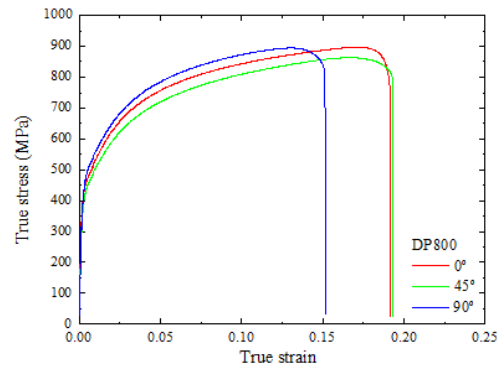| Angle (degrees)	σ_y (MPa)	σ_u (MPa)	ε_u (%)	ε_T (%)	n	R
0	450.77	866.74	12.7	18.5	0.166	0.579
	3.02	8.26	0.2	0.6	0.001	0.018
45	441.06	863.66	13.6	19.9	0.173	1.077
	7.04	16.66	0.3	0.6	0.001	0.095
90	482.75	886.95	11.0	15.0	0.161	0.696
	3.40	3.51	0.2	0.2	0.001	0.020

Fig. 7 Uniaxial tensile true stress-strain curves of DP800 steel

B. Hydraulic Bulge Test

The strain-hardening behaviour of both DP600 and DP800 steel sheets under hydraulic bulge conditions can be analysed in Fig. 8 where the equivalent stress and equivalent plastic-strain measures are plotted. DP800 steel grade provided higher flow stress behaviour with an ultimate equibiaxial yield strength close to 1,000 MPa in detriment to the equivalent plastic-strain value which maximum value is near to 0.45. As in [10] and [11], AHSS with higher martensite volume fraction content are prone to fracture propagation inside the harder phase increasing the stress level and decreasing the ductility. Conversely, in DP600 steel grade lower stress levels are associated with the softer ferrite-martensite interface with coarse undeformed martensite islands, thus, allowing to higher strain gradients in comparison to DP800 grade. The corresponding fitted parameters according to Swift's work-hardening law, defined in (1), are given in Table III. These parameters were adopted in the numerical predictions for the limit strains of both DP600 and DP800 steel sheets.

TABLE III
UNIAXIAL MECHANICAL PROPERTIES OF DP800 STEEL SHEET

Steel	K (MPa)	ε_0 (%)	n
DP600	1,067.2	0.2	0.192
DP800	1,185.5	0.2	0.168

World Academy of Science, Engineering and Technology
International Journal of Materials and Metallurgical Engineering
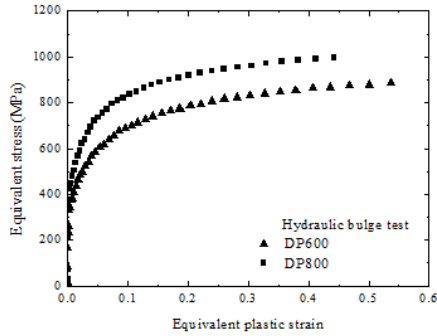Vol:9, No:9, 2015

Fig. 8 Equivalent stress and equivalent plastic-strain curves obtained from bulge testing of DP600 and DP800 steel sheets

C. Forming Limit Curve (FLC)

Fig. 9 shows the deformed Forming Limit Curve (FLC) specimens for both DP600 and DP800 steels. It is worth to observe that most of the fractured sites are located very close to the specimen pole. Also, wrinkles were formed in the edges of 180 mm and 220 mm specimens, indicating that the blank-holder load must be increased for these geometries. However, no sliding was detected in the deformed blanks thanks to the stretching conditions imposed by the circular lockbead.


(a)

(b)

Fig. 9 Deformed FLC specimens according to Nakajima's procedure:
(a) DP600 and (b) DP800 grades

The experimental limit strains of DP600 and DP800 steels are plotted in Fig. 10 for both necking (ISO 12004-2:2008) and fracture conditions indicated by filled and open symbols, respectively. The corresponding forming limit curves were obtained by joining the strain data in order to define the lowest limit strains. As expected, DP800 sheet showed lower forming

limits than the limit strains determined for DP600 steel grade. In addition, the plane-strain intercept, namely, the FLC_0-values obtained at necking condition of both steels are consistent with the average strain-hardening exponents, see Tables I and II, $\bar{n}_{90} = 0.194$ ($FLC_0 = 0.184$) and $\bar{n} = 0.168$ ($FLC_0 = 0.163$) for DP600 and DP800 steels, respectively.
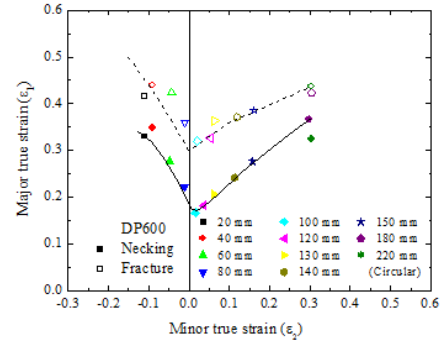
(a)
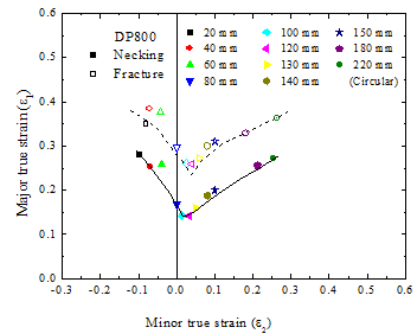
(b)

Fig. 10 Experimental Forming Limit Curves at necking and fracture:
(a) DP600 and (b) DP800

D. Numerical Predictions

Fig. 11 compares the experimental limit strains determined at the necking condition for both dual-phase steels with the numerical predictions of the present elasto-plastic M-K model. The material parameters in Ferron's criterion were identified from the average plastic anisotropy R-values determined in uniaxial tensile tests, see Tables I and II. The initial value of the M-K model geometrical imperfection f_0 was set equal to 0.997. The numerical predictions provided a good agreement with the experimental FLC_0-values of both DP600 and DP800 steels. However, the M-K model numerical predictions overestimated and underestimated the corresponding experimental limit strains in the biaxial stretching and drawing regions of the FLC.

These discrepancies can be accredited to the localized necking condition criterion adopted in the M-K modelling which usually provides realistic predictions for thin metallic sheets under ductile fracture wherein a necking growth condition prevails.

World Academy of Science, Engineering and Technology
International Journal of Materials and Metallurgical Engineering
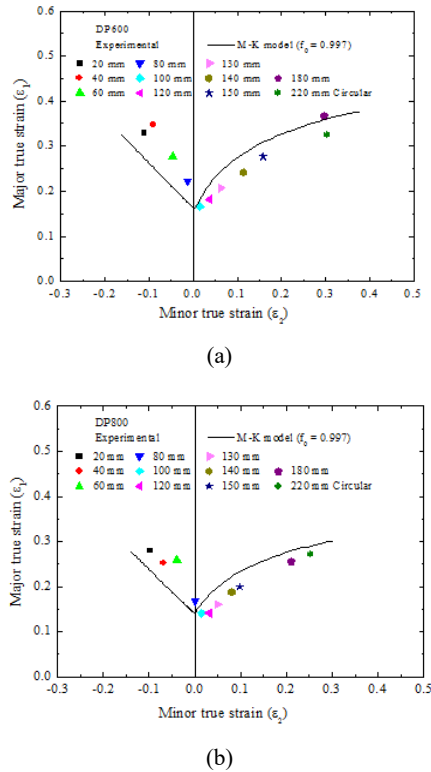Vol:9, No:9, 2015

(a)

(b)

Fig. 11 Comparison between the numerical and experimental limit strains: (a) DP600 and (b) DP800

Recently, the plastic behaviour of DP600 steel sheet was analysed in [12] by means of Nakajima's FLC procedure, scanning electron microscopy (SEM) surface fracture analysis and FE simulations in order to identify the failure mechanisms causing the fracture of this AHSS grade. From SEM analysis three failure types in DP600 sheet were classified in [12], namely, (i) plastic instability across the thickness and ductile fracture under (ii) tensile and (iii) shear stress states conditions. The FLC specimens for which the limit strains were found to be near to equibiaxial stretching deformation mode ($\varepsilon_1 = \varepsilon_2$), the main failure mechanism detected is ductile tensile fracture. Conversely, some FLC specimen geometries situated between the biaxial stretching ($\varepsilon_1 \neq \varepsilon_2 > 0$) and the plane-strain intercept ($\varepsilon_2 = 0$) showed a ductile shear fracture whereas the specimens which provided limit strain values in the FLC drawing range ($\varepsilon_1 > 0 \neq \varepsilon_2 < 0$) displayed a thickness plastic instability, which is consistent with the localized necking in thin sheets. Thus, a unique localized necking condition will not provide an accurate prediction of both drawing and biaxial stretching regions of the experimental FLC observed for AHSS sheets. More complex failure criteria recently proposed to describe the behaviour of AHSS sheets [13], [14] will be investigated in future works.

The predicted Forming Limit Stress Curves (FLSC's) are plotted in Fig. 12 in the principal stress space (σ_1, σ_2) together with the average experimental values of the uniaxial tensile ultimate yield strength determined at 0 and 90 degrees with respect to the rolling direction. The predictions of the principal strains overestimate the experimental uniaxial ultimate yield

strength values of both DP600 and DP800 sheets, as indicated by the uniaxial tension values determined for $(0, \sigma_1)$ and $(\sigma_2, 0)$ stress states which are along the in-plane axes of orthotropy aligned with the transverse and rolling directions, respectively. Actually, these higher limit stresses values explain the lowered limit strains predictions obtained between the plane-strain intercept (FLC$_0$-value) and the drawing region ($\varepsilon_1 > 0, \varepsilon_2 < 0$) of the FLC, as shown in Fig. 11.
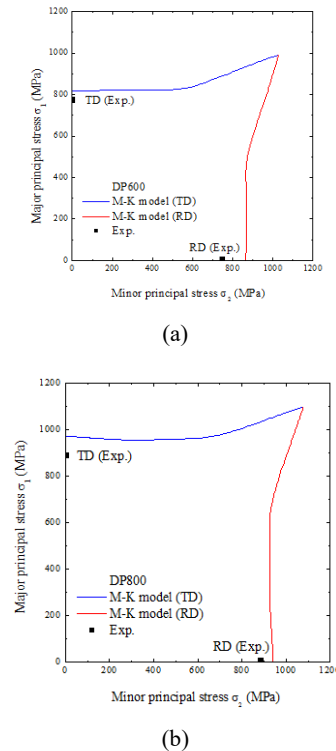

(a)

(b)

Fig. 12 Forming limit stress predictions: (a) DP600 and (b) DP800

V. CONCLUSIONS

In this work, the plastic behaviour of two AHSS sheets DP600 and DP800 grades was firstly evaluated by means of mechanical tests, namely, uniaxial tensile and hydraulic bulge. Afterwards, the forming limits at both necking and fracture conditions were defined according to the Nakajima's Forming Limit Curve (FLC) procedure using a hemispherical punch. Moreover, an elasto-plastic localization model is proposed to forecast the limit strains assuming a localized necking criterion. From the corresponding experimental and numerical results, the following conclusions can be summarized as:

(1) The plastic behaviour in uniaxial tension of both dual-phase steels DP600 and DP800 showed similar yield strength values angular orientation dependence, namely, $\sigma_{90} > \sigma_0 > \sigma_{45}$, and a corresponding ductility behaviour given by total strain values $\varepsilon_{45} > \varepsilon_0 > \varepsilon_{90}$;

(2) The strain-hardening behaviour of DP600 and DP800 sheets under hydraulic bulge test at large strains conditions allowed to obtain an optimized fit for the parameters of an empirical work-hardening equation;

World Academy of Science, Engineering and Technology
International Journal of Materials and Metallurgical Engineering
Vol:9, No:9, 2015

(3) The experimental limit strains at necking and fracture conditions obtained according to Nakajima's procedure showed a rather good formability level for both DP600 and DP800;

(4) The numerical predictions of the limit strains at necking obtained with the proposed M-K localization model provided the same trend of the experimental values in the drawing region of the Forming Limit Curve along with a good forecast of the plane-strain intercept FLC_0-value obtained for both DP600 and DP800 steels.

(5) The usual localized necking criterion adopted in the M-K model overestimated and underestimated the limit strains in the biaxial stretching and drawing FLC regions of both dual-phase steels, respectively. In the biaxial stretching domain, failure in AHSS sheets are more likely to occur by ductile shear and ductile tensile fracture mechanisms;

The Forming Limit Stress Curve predictions determined for both dual-phase sheets overestimated the experimental uniaxial ultimate yield strength values at 0 and 90 degrees with respect to the rolling direction. In fact, the proposed MK-model approach forecasted higher limit stress levels which explain the lowered limit strains predictions determined between the plane-strain intercept and the drawing FLC region.

ACKNOWLEDGMENT

REFERENCES

[1] Gan, Y., Advanced Steel and Our Society: Better Steel, Better World, "Advanced Steels: The Recent Scenario in Steel Science and Technology," Eds, Weng, Y., Dong, H, Gan, Y., German. Metallurgical Industry Press, Beijing and Springer-Verlag GmbH Berlin Heidelberg, 2011.
[2] S.P. Keeler, W.A. Backofen, "Plastic instability and fracture in sheets stretched over rigid punches," ASM Trans. Quart. 56, 25, 1964.
[3] G.M. Goodwin, "Application of strain analysis to sheet metal forming problems in press shop," SAE Paper No. 680093, 1968.
[4] R. Hill, "On discontinuous plastic states, with special reference to localized necking in thin sheets," J. Mech. Phys. Solids 1, 1952.
[5] Z. Marciniak, K. Kuckzynski, "Limit strains in the processes of stretch-forming sheet metal," Int. J. Mech. Sci. 9, 1967, pp. 609–620.
[6] M. Koç, E. Billur, O.N. Cora, "An experimental study on the comparative assessment of hydraulic bulge test analysis," Materials and Design 32, 2011, pp. 272–281.
[7] R. Hill, "A theory of plastic bulging of a metal diaphragm by lateral pressure", Philos. Mag. Series 7 40, 1950, pp.1133-1142.
[8] M. M. C. S. Freitas, L. P. Moreira, R. Garcez, "Experimental analysis and theoretical predictions of the limit strains of a hot-dip galvanized interstitial-free steel sheet," Materials Research 16, 2013, pp. 351-366.
[9] G. Ferron, R. Makkouk, J. Morreale, A parametric description of orthotropic plasticity in metal sheets, International Journal of Plasticity, Vol. 10, 1994, pp. 431-449.
[10] W. Wang, X. Wei, "The effect of martensite volume and distribution on shear fracture propagation of 600-1000 MPa dual phase sheet steels in the process of deep drawing". International Journal of Mechanical Sciences, Vol. 67, 2013, pp. 100-107.
[11] A. Saaia, O.S. Hopperstad, Y. Granbom, O.-G. Lademo, "Influence of volume fraction and distribution of martensite phase on the strain localization in dual phase steels," 20th European Conference on Fracture (ECF20), Procedia Materials Science 3, 2014, pp. 900 - 905.
[12] O. Björklund, L. Nilsson, 'Failure characteristics of a dual-phase steel sheet," Journal of Materials Processing Technology, 214, 2014, pp. 1190–1204.
[13] L. Yaning, L. Meng, G. Jörg, W. Tomasz, "Prediction of shear-induced fracture in sheet metal forming," Journal of Materials Processing Technology, 210, 2010, pp. 1858–1869.
[14] L.Yanshan, H. Lou, "Prediction of ductile fracture for advanced high strength steel with a new criterion: Experiments and simulation," Journal of Materials Processing Technology 213, 2013, pp. 1284– 1302.

M. C. Cardoso was born in Niterói, Rio de Janeiro state, Brazil, 1972. He graduated from Civil Engineering at Veiga de Almeida University, Rio de Janeiro, in 1990. He received the title of Master of Sciences in Metallurgical Engineering in 2012 at Federal Fluminense University, Volta Redonda, Rio de Janeiro state, Brazil. Now, he is a PhD. student at the same university with a scholarship from CAPES foundation. His thesis subject is about the plastic behaviour of advanced high strength steels.

L. P. Moreira received his 'Docteur en Sciences' in Mechanics of Materials from Metz University in 2002. He is currently Associate Professor at the Department of Mechanical Engineering, Federal Fluminense University, Volta Redonda, and Rio de Janeiro, Brazil. His research interests include the modelling and simulation of metal forming processes.